JOURNAL OF GEOPHYSICAL RESEARCH, VOL. 114, A05204, doi:10.1029/2008JA013682, 2009

A comprehensive high-throughput analysis of substorms observed by IMAGE magnetometer network: Years 1993–2003 examined

E. I. Tanskanen[1,2]

Received 13 August 2008; revised 29 December 2008; accepted 23 January 2009; published 8 May 2009.

[1] The annual and yearly variation of the substorm activity during a complete solar cycle, from year 1993 to year 2003, has been examined. Almost 6000 substorms were identified by an automated search engine. The identification method was found to be robust and applicable to all activity levels. To examine the long-term (annual, yearly, and solar cycle) variability in the substorm occurrence rate, we formed a measure called the substorm number. The substorm number and peak amplitude were found to only weakly follow the Sun's activity measured by a sunspot number. During the years of sunspot maxima in the solar cycle 23, the Northern Hemisphere auroral region was only moderately active. The largest substorm numbers and peak amplitudes were found during the declining solar cycle phases when the interplanetary high-speed streams hit the Earth. We found out that the substorms last longer during the least active season (i.e., summer months) and during the least active years (e.g., 1997 and 2001). Furthermore, the substorm number and peak amplitude show much larger values for winter than for summer, which may be partly due to the fact that the maximum southward component of the interplanetary magnetic field (B_{south}) occurs in February and the minimum occurs in June.

Citation: Tanskanen, E. I. (2009), A comprehensive high-throughput analysis of substorms observed by IMAGE magnetometer network: Years 1993–2003 examined, *J. Geophys. Res.*, *114*, A05204, doi:10.1029/2008JA013682.

1. Introduction

[2] The auroral substorms are one of the two main appearances of geomagnetic activity [*Birkeland*, 1908; *Akasofu*, 1964; *McPherron*, 1979], the other being the magnetic storms [e.g., *Chapman and Bartels*, 1940]. Historically, the changes in the terrestrial substorm activity have been examined by visual investigation of observations of aurora. The first reported scientific observations of substorm-like features were made in 1838 by E.C. Herrick [*Siscoe*, 1980]. Since then substorms have been identified from many different scientific measurements: from keograms based on ground-based all-sky camera images [e.g., *Akasofu*, 1964], from VIS and FUV images on board spacecraft [e.g., *Frey et al.*, 2004; *Østgaard et al.*, 2007], magnetic field measurements from the ground [e.g., *Birkeland*, 1908; *Akasofu*, 1964] and from the space.

[3] Despite the long history of substorm investigations only a few large statistical substorm studies have been published. The largest existing substorm databases are presented by *Borovsky et al.* [1993], *Tanskanen et al.* [2002, 2005], *Newell et al.* [2001], and *Frey et al.* [2004]. *Borovsky et al.* [1993] identified about 1500 substorms on the basis of particle injections monitored by three geosynchronous satellites. *Tanskanen et al.* [2002, 2005] identified substorms from auroral region ground-based magnetic observations: about 840 substorm in 1997 and 1999 [*Tanskanen et al.*, 2002] and over 5000 substorms between 1993 and 2003 [*Tanskanen et al.*, 2005]. *Newell et al.* [2001] examined 390 substorms identified from POLAR UV Imager, and *Frey et al.* [2004] found more than 2400 substorm onsets over the 2.5 years of operation of FUV instrument on board the IMAGE spacecraft.

[4] Traditionally, the substorm events have been identified manually or semimanually from ground-based or spaceborne observations. In this paper we identify large number of substorms by using the search engine. The automated search engines have been successfully used to identify, e.g., genetic patterns in biology [*Durbin et al.*, 1998] and auroral forms from all-sky camera images in space physics [*Syrjäsuo and Donovan*, 2004]. The substorm events can be identified algorithmically following the mathematically formed identification algorithm. That requires that substorms can be defined precisely. The substorm definition is mechanistic and precise when the substorm evolution follows a certain mechanism. For substorm identification that requires that a substorm can be formed of: (1) a growth phase with a start point, (2) an expansion phase with an onset indicator followed by a peak activity, and (3) a recovery phase with an end point (see Figure 1). This kind of substorm definition enables algorithmic identification of substorm events.

[5] The existing long-term substorm studies over the several months, years and solar cycles have been carried out by forming various activity indices and analyzing their trends, while the short-term studies have been usually carried out by identifying the individual substorm events. The

[1]Department of Physics and Technology, University of Bergen, Bergen, Norway.
[2]Also at Finnish Meteorological Institute, Helsinki, Finland.

0148-0227/09/2008JA013682$09.00

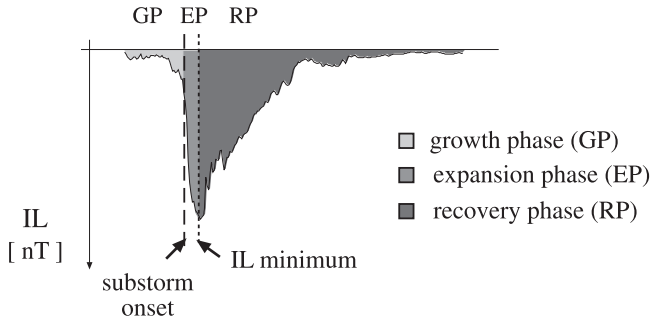

Figure 1. A sketch of a substorm event showing the substorm phases: a growth phase, an expansion phase, and a recovery phase.

activity indices such as *AE*, *Kp*, *aa* and *PC* index can be, and have been, successfully used to measure the geomagnetic activity in the different parts of the globe and with different time scales. The longest time series is from 1 h aa [*Mayaud*, 1973], which can be used back to 1868 [*Cliver et al.*, 2002], or based on single station observations back to 1844 [*Nevanlinna and Kataja*, 1993]. The 3-h *Kp* index is used to estimate the overall geomagnetic activity level, and *PC* index in 1 h resolution is used to measure the polar cap magnetic activity. The 1 h auroral electrojet indices (*AU*/*AL*) were introduced as measures of global electrojet activity at the northern hemisphere auroral oval [*Davis and Sugiura*, 1966]. Both *AU* and *AL* indices are derived from geomagnetic variations in the horizontal magnetic field component, observed at the selected 10–13 observatories along the auroral zone in the northern hemisphere. The strength of the westward and eastward auroral electrojets are reflected in *AL* and *AU* indices, respectively. Several electrojet indices in the local UT sectors, including *CU*/*CL* from Canopus [*Rostoker et al.*, 1995] and *IU*/*IL* [*Kallio et al.*, 2000] from the IMAGE network [*Viljanen and Häkkinen*, 1997] have been created, because of their better coverage of the maximum disturbance [*Kauristie et al.*, 1996]. In this paper, the substorms have been identified from the IL index in 60 s resolution, which covers the UT interval about from 1600 UT to 0300 UT the next day.

[6] The terrestrial magnetic activity is known to be driven by the geoeffective solar wind structures such as shocks, and interplanetary coronal mass ejections [e.g., *Richardson et al.*, 2000; *Koskinen and Huttunen*, 2006], and roughly follow the Sun's magnetic activity cycle, the sunspot cycle. The northern hemisphere (equatorial) magnetic activity is reported to increase and decrease following the Sun's magnetic activity measured by a sunspot number, such that the strongest (weakest) activity exists during the sunspot maximum (minimum) [see, e.g., *Cliver et al.*, 2002]. The auroral region magnetic activity is, however, suggested to peak during the declining solar cycle phases [*Tsurutani et al.*, 1995; *Nevanlinna and Pulkkinen*, 1998], roughly 3–4 years after the sunspot maximum [*Tanskanen et al.*, 2005].

[7] The seasonal variation of the geomagnetic activity has been studied for years [*Currie*, 1966; *Russell and McPherron*, 1973]. It is well known that the geomagnetic activity is enhanced during the spring and fall equinoxes because of the three external drivers: the Russell-McPherron effect [*Russell and McPherron*, 1973], the equinoctial effect [*Bartels*, 1925] and the heliographic latitude [*Cortie*, 1912]. However, little is known about the seasonal variation of the actual substorm events. In particular, the seasonal variation of the substorm occurrence rate, peak amplitude and duration have so far been left unstudied.

[8] For the purpose of this paper and to enable further short-term and long-term substorm studies, we have created a mechanistic substorm definition (chapter 2) and tested a substorm search engine called the SSeeker. We examine the yearly and seasonal variation of substorms over a complete solar cycle (1993–2003), with a database consisting of almost 6000 substorms identified by the SSeeker. We show the solar cycle variation for substorm occurrence rate, for the peak amplitude and for the substorm duration (chapter 4) together with the superposed epoch curves of substorms with different onset drop and zero epoch criteria (chapter 5). The seasonal variation of the peak substorm amplitude, of the substorm duration, and of the occurrence rate is shown in chapter 6. Furthermore, we form a measure called the substorm number, R_{ss}, which can be used to describe the long-term trends in the terrestrial substorm activity.

2. Substorm Database

[9] We identified and examined all substorms in the UT sector 1600–0300 UT over a complete solar cycle from years 1993 to 2003. The solar cycle 23 began on May 1996 and peaked on April 2000, while the previous solar cycle 22 began on September 1986 and peaked on August 1990. The IL index [*Kallio et al.*, 2000] is created from the IMAGE network [*Viljanen and Häkkinen*, 1997; *Syrjäsuo et al.*, 1998] magnetic measurements in the northern hemisphere auroral region, from which we identified 5914 substorms.

2.1. IL Index Formation

[10] The IL index is constructed by computing an envelope of the north–south magnetic field components of the IMAGE measurements [*Kallio et al.*, 2000]. The baselines, necessary for the envelope computation, were visually selected from the IMAGE data. The most quiet period during each day, lasting between 15 and 60 min, was selected to determine the baseline. If there was no quiet period during a day, baseline from one of the previous or the next few days was used.

[11] An example substorm on 8 July 1997 is shown in Figure 2. Substorm usually begins with a slow growth phase lasting up to an hour [*Kallio et al.*, 2000]. The onset starts an expansion phase including a rapid decrease in the IL index followed by a slow recovery back to the presubstorm IL values. The IMAGE magnetometer network used in this paper has a magnetometer at about every 100 km from 60° to 80° geographic latitude, except for the about 500 km gap between Sørøya and Bear Island observatories over the Arctic ocean. The IMAGE network gives an excellent latitudinal coverage and enables capturing of the substorms during all geomagnetic activity levels.

2.2. Substorm Identification and Search Engine SSeeker

[12] To enable a high-throughput identification of substorms, which is required to study a large number of events, a mechanistic method of substorm identification was developed. In this study, we used the following identification method.

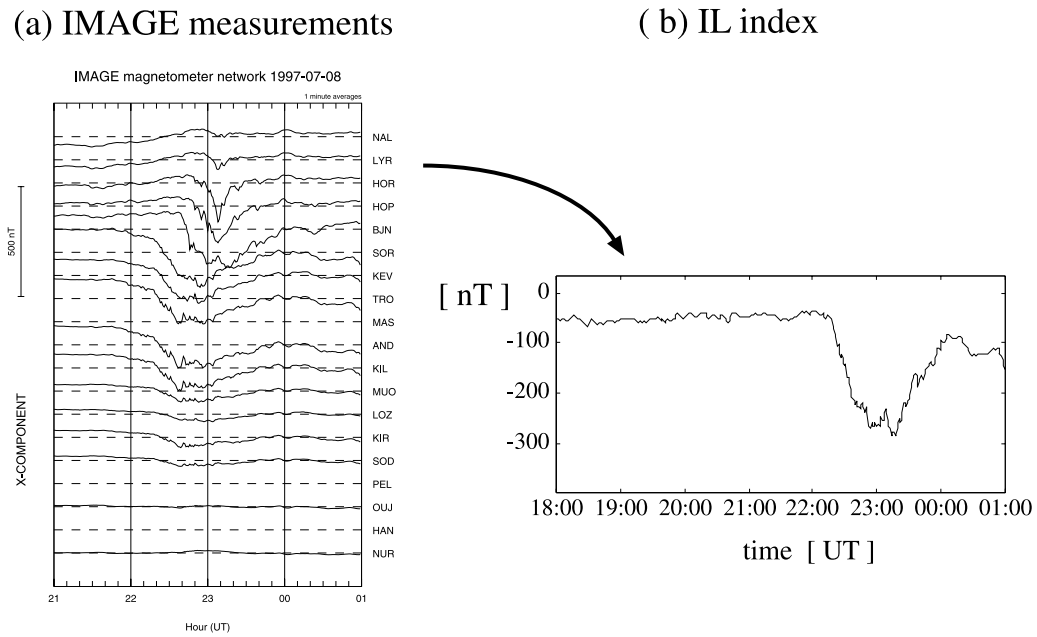

Figure 2. An example substorm event on 8 July 1997 at 2100–0100 UT. (a) Observations of the north–south component (x component) of all IMAGE magnetometers. (b) An IL index created as an envelope curve of the x components of the B field measured by all of the IMAGE magnetometers.

[13] 1. The IL index was formed as described above.

[14] 2. The main substorm onset was sought by searching a rapid decrease, more than 80 nT in 15 min, leading to negative bay development. The substorm onset time is defined to be the time when the first sign on the 80 nT in 15 min drop appears.

[15] 3. The substorm was defined to begin when the first signs of the negative bay development showed up (the IL index close to zero). However, the beginning of the substorm was restricted to occur at most 30 min. before the substorm onset.

[16] 4. The event was considered to end when the IL index recovered to two tenths of the peak amplitude. The new substorm was combined to the previous one if it began less than 10 min after the end of the previous substorm.

[17] The method described above was implemented as the substorm search engine SSeeker. Substorm candidates were rejected if they were shorter than 15 min, if the peak amplitude of the event was smaller than 100 nT or if they began before 1600 UT or after 0300 UT, which is not the IMAGE optimal coverage period. The mechanistic substorm definition given above is robust and was verified to be applicable to the IL data during all activity levels.

3. Substorm Number

[18] The substorm number is defined to be the number of substorms in a certain time interval (e.g., during a year or a month). The substorm number will be used to describe the substorm occurrence rate, analogously to the sunspot number, which has been used to describe the number of sunspots (or sunspot groups) over the 300 years. A total of 5914 substorms were found during 11 years examined, which gives a substorm number 5914.

[19] The yearly variability of substorm number was large. The largest yearly substorm number (699) was for 2003, and the smallest substorm number (452) was for 2001 (Figure 3b). The lowest substorm numbers were observed during the year of the sunspot maximum of the solar cycle 23, while the largest occurrence rate was about 3 years after the sunspot maximum. The same trend holds for the previous solar cycle 22 as well. The yearly substorm number for 1994 was 630, which is only slightly less than for 2003 (699), but dramatically more than for any other year between 1993 and 2003. Thus, the substorm number does not correlate with the sunspot number, but instead the substorm number follows the high-speed stream activity, which is known to peak 3–4 years after the solar maximum [*Tanskanen et al.*, 2005].

4. Substorm Strength and Duration

[20] A substorm can grow up to several thousand nanoteslas, which usually happens when a magnetic storm is in process. In this paper, the substorm strength (or size) is defined as the absolute value of the peak substorm amplitude, i.e., the minimum *IL* index during the event. The substorms occurring during the Halloween storm [*Baker et al.*, 2004] on early November 2003 were the largest observed during the examined time interval, over 4000 nT in size. Average substorm size in this data set is 396 nT with the standard deviation of 54 nT. The smallest substorms occur in 1997 (yearly average 315 nT) and the largest, on average, during years 1994 and 2003 (493 and 487 nT, respectively) (Figure 4).

[21] The annually averaged substorm duration varies from 2 h 45 min to 3 h 20 min, the average being 3 h 5 min (with standard deviation 12 min) (Figure 5). The longest substorm events, on average, were observed in 2003 (3 h and 20 min) and 1994 (3 h and 15 min), while the shortest substorms are in 1993 (2 h and 42 min) and 1997 (2 h and 45 min). Roughly one fourth of the substorms last longer than 4 h and one fourth last less than 1.5 h, when 15 min is used as a minimum length

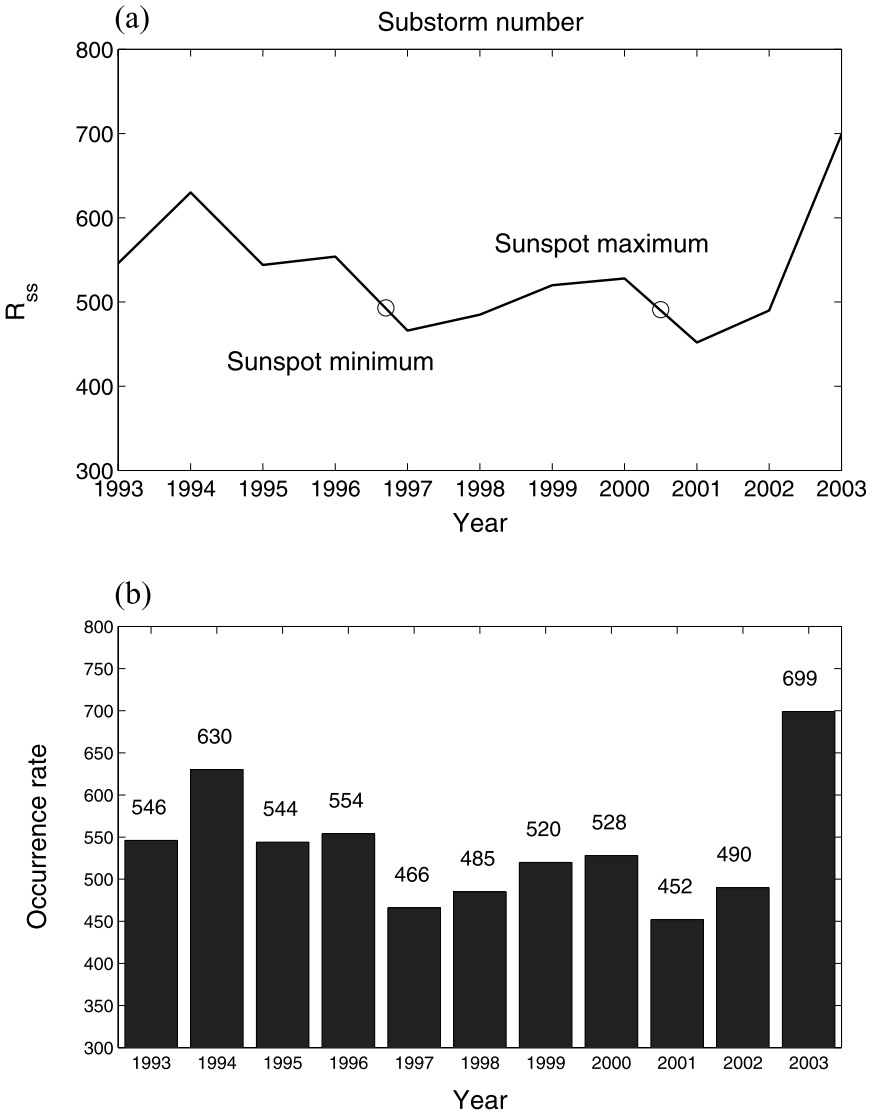

Figure 3. (a) The yearly substorm number R_{SS}, which characterizes the substorm occurrence rate in the Earth's magnetosphere. The substorm number is shown for years 1993–2003. (b) The yearly substorm number in a histogram format.

criteria (Figure 5). Furthermore, about 13% of the substorms last less than an hour.

5. Typical and Unusual Substorm Signatures

[22] A superposed epoch curve was formed separately for each year from 1993 to 2003. In the first case, the zero epoch time was set to be the time of the substorm onset (Figure 6), and in the second case the zero epoch time was set to be the peak amplitude (Figure 7). In Figure 6 we show superposed epoch curves for 1994, 1996, 2001 and 2003 (marked with blue, green, black and red color, respectively). When the zero epoch time is set to be at the onset, the superposed epoch curves show a rather flat growth phase followed by a negative bay lasting up to 2–4 h depending on the definition of the substorm end point (Figure 6). The superposed epoch peak amplitude is roughly 6 min after the midnight, which agrees very well with the peak auroral power given by POLAR UVI statistics [*Newell et al.*, 2001]. In this paper, we defined substorm to end when the substorm had recovered about to two tenths of the peak amplitude value. The end point of the substorm does not show clearly in the superposed epoch plots in Figure 6, since the duration of the events are not scaled, but the real duration of the substorms are shown.

[23] To study how the form of the superposed epoch curve changes when the more strict selection criteria for the drop time is used, we select two subgroups of substorms (A and B). For the subgroup A ("medium-sized" and "large" substorms) we require that the onset drop is more or equal to 20 nT/min lasting longer than 15 min, which is 300 nT drop in 15 min. For the subgroup B (large substorms) we require 30 nT/min drop lasting longer than 15 min (equal to 450 nT/15 min). In a subgroup A we have 249, 133, 101 and 254 substorms (1994, 1996, 2001 and 2003, respectively), while in a subgroup B we have 127, 53, 49 and 116 substorms (1994, 1996, 2001 and 2003, respectively). The original occurrence rate of substorms were 630, 554, 452 and 699 (1994, 1996, 2001 and 2003, respectively). The peak amplitude for

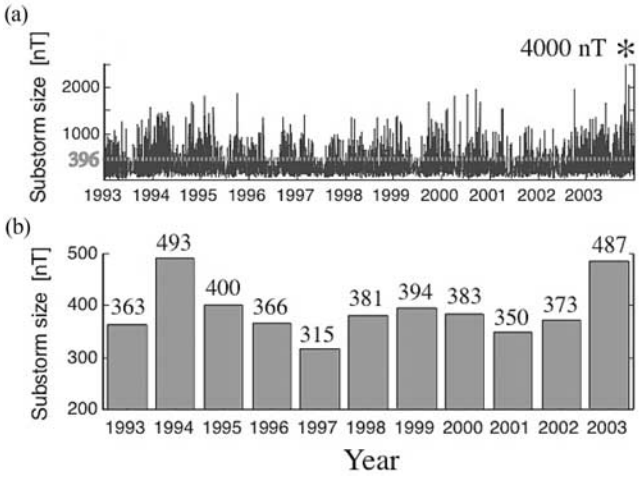

Figure 4. (a) The strength (peak amplitude) of each substorm identified for years 1993–2003. (b) Yearly averaged strength, showing the tendency of having stronger substorms during the declining solar cycle phases.

subgroup B substorms (Figure 6c) vary from −650 nT for substorms occurring in 1996 to −750 nT for the year 2003 substorms. The peak amplitude for subgroup A substorms vary from −450 nT (for 1996) to −550 nT (for year 2003).

[24] The typical substorm obtained through the superposed epoch analysis shows a slow increasing trend in an activity level during the substorm growth phase (i.e., the *IL* index decreases). The increasing trend during the substorm growth phase is more clear for the medium-sized and large substorms (subgroups A and B) and less clear for small substorms. However, just before the substorm onset the activity level decreases briefly (i.e., the *IL* index increases). Whether this dip is real or due to the method of forming the superposed epoch curves, is not known.

[25] For the medium-sized and large substorms (subgroups A and B) the recovery phase usually lasts about 2.5 h (Figures 6b and 6c), while for small substorms the recovery phase lasts longer (cannot be identified precisely from Figure 6a). The shape of the superposed epoch curve during the recovery phase show a slight yearly variation, such that for some years (e.g., 2001) substorms recover sooner than for the other years (e.g., 2003). The more strict drop selection criteria we use, the better the superposed epoch plot looks like so-called "typical substorm" (Figure 6). In addition, it looks like for more magnetically active years also the background activity level is larger than for more magnetically quiet years. It means that the identification of the individual substorms, particularly during the very active years, can be difficult if the baseline selection is not done properly. We suggest that the baseline selection should be done in daily basis whenever possibly.

[26] The zero epoch time in superposed epoch curves have traditionally been selected to substorm onset. However, then the substorm return times (i.e., recovery phase duration) cannot been properly compared to the drop time duration. In Figure 7 we show superposed epoch curves with zero epoch time selected to peak substorm amplitude instead of the substorm onset. The return time from the maximum peak amplitude (not from the peak of the first expansion) to the quiet time activity level is two times longer than the drop time to the peak maximum amplitude for the entire substorm data set (Figure 7). For subgroups A and B the return time is

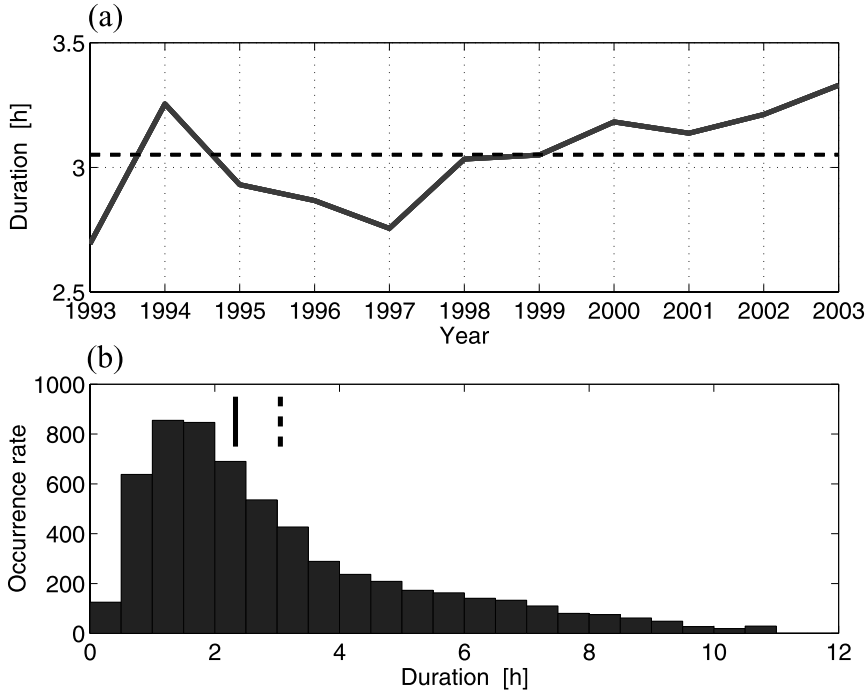

Figure 5. (a) The yearly averaged substorm duration for years 1993–2003. The average duration is 3 h and 5 min. (b) A substorm duration for substorms from 1993 to 2003 binned by 30 min bins. The mean (3 h and 5 min) and median (2 h and 20 min) are marked by a dashed vertical line and a solid vertical line, respectively.

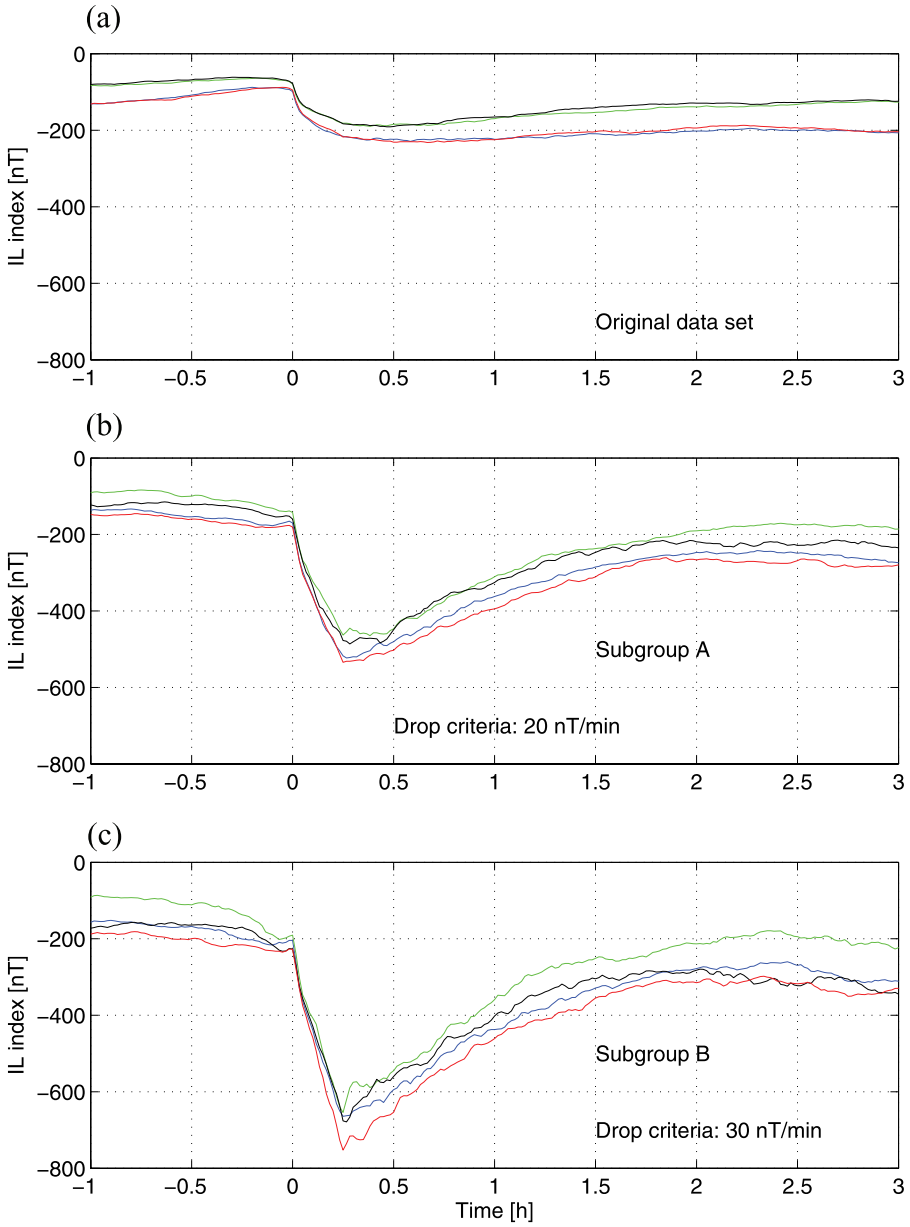

Figure 6. Superposed epoch curves where the substorm onset is selected to be a zero epoch time. Superposed epoch curves for 4 years are shown with a color coding: 1994 (blue), 1996 (green), 2001 (black), and 2003 (red). (a) An entire data set with an onset drop criteria 80 nT/15 min, which is about 5 nT/min. (b) Medium-sized and large substorms (subgroup A) with an onset drop criteria 20 nT/min. (c) Large substorms (subgroup B) with an onset drop criteria 30 nT/min.

three times longer than the drop time to the peak substorm amplitude, indicating that large substorms have longer recovery phases than small substorms.

6. Seasonal Variation of Substorms

[27] The seasonal variation of the substorm number, duration and substorm strength was examined for the entire substorm data set of 5914 substorms. Strongest substorms occur during spring and fall, while the weakest substorms occur at summer and winter months. The substorms in June are clearly weaker than the substorms in February (Figure 8). That may be partly due to the fact that the maximum southward component of the interplanetary magnetic field (B_{south}) occurs in February and minimum in June [*Newell et al.*, 2002; *Cliver et al.*, 2000].

[28] Surprisingly, more substorms occur during winter (November, December, and January) than summer months (May, June, and July), and fall (August, September, and October) than spring months (February, March, and April). It is not known why this is the case. However, the seasonal variation of the substorm duration agrees very well with the seasonal variation of the substorm number. The longest substorms occur in summer months and the shortest substorms occur during winter time, when the new substorm often cuts

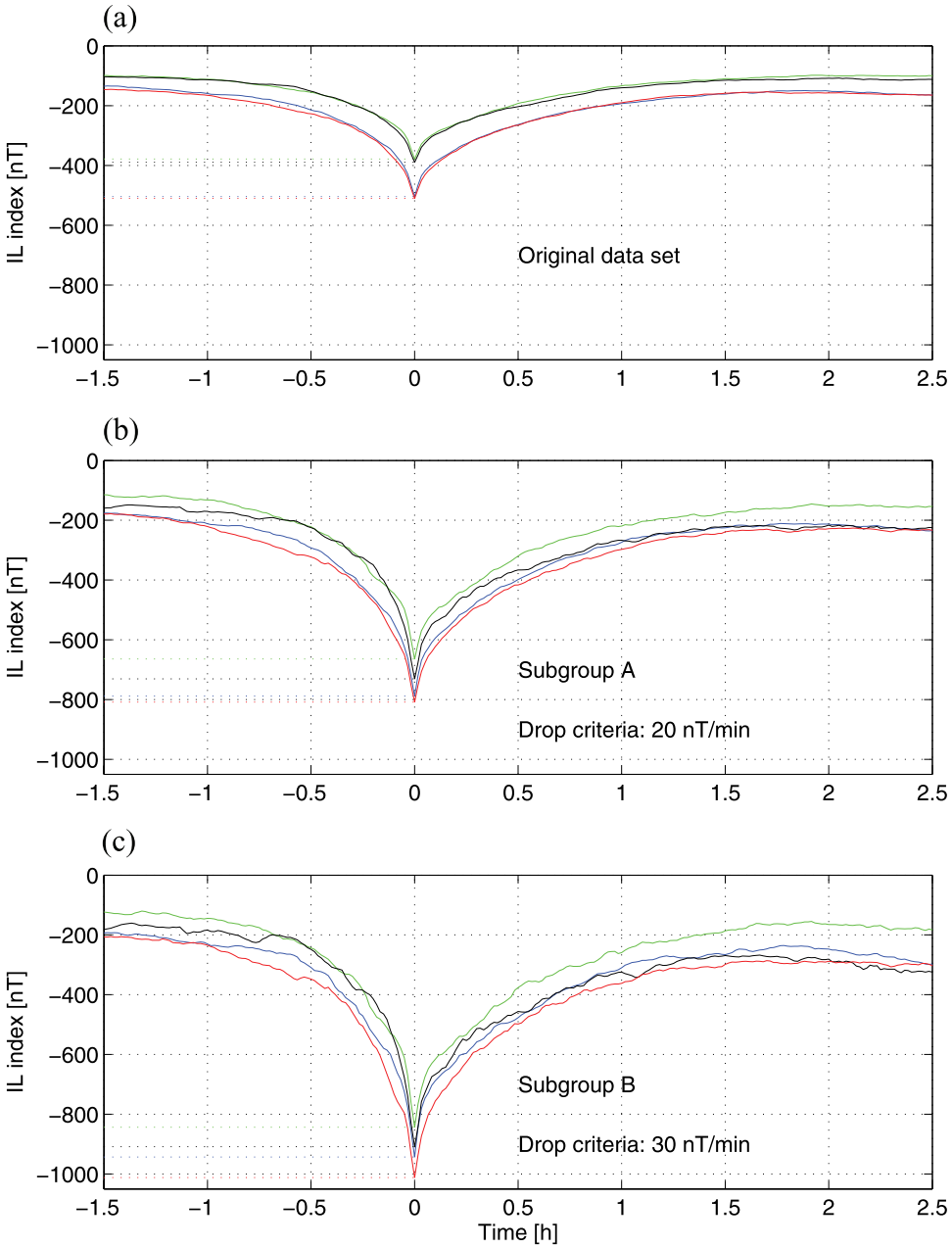

Figure 7. (a–c) Superposed epoch curves where the zero epoch time is a peak substorm amplitude. A color coding and subgroup selection in the same way as in Figure 6.

the previous substorm and leaves it shorter than substorms during other seasons.

7. Discussion

[29] The results of the comprehensive substorm analysis show that substorms during different years and months have clearly different average characteristics. The substorm occurrence rate, peak amplitude and duration has an annual and sunspot cycle variation, which has been presented in this paper.

[30] As a check of the algorithmical search concept, the substorms found using the method described in chapter 2.2 were compared to substorms obtained for years 1997 and 1999 using the same *IL* index [*Tanskanen et al.*, 2002]. The list of substorms identified by SSeeker was in good agreement with the list of manually identified substorms [*Tanskanen et al.*, 2002]; the differences were mainly due to use of additional data in manual search, such as the interplanetary magnetic field B_z component. In this paper, we did not require interplanetary magnetic field data to be available for substorm identification as was required in the work by *Tanskanen et al.* [2002].

[31] In this paper, the ground-based magnetic field measurements are used to identify the substorms, because that data gives much better coverage than any other instrument capable of measuring the substorms. However, substorms over short time intervals (days and months) can be identified on the basis of several other measurements, too, e.g.,

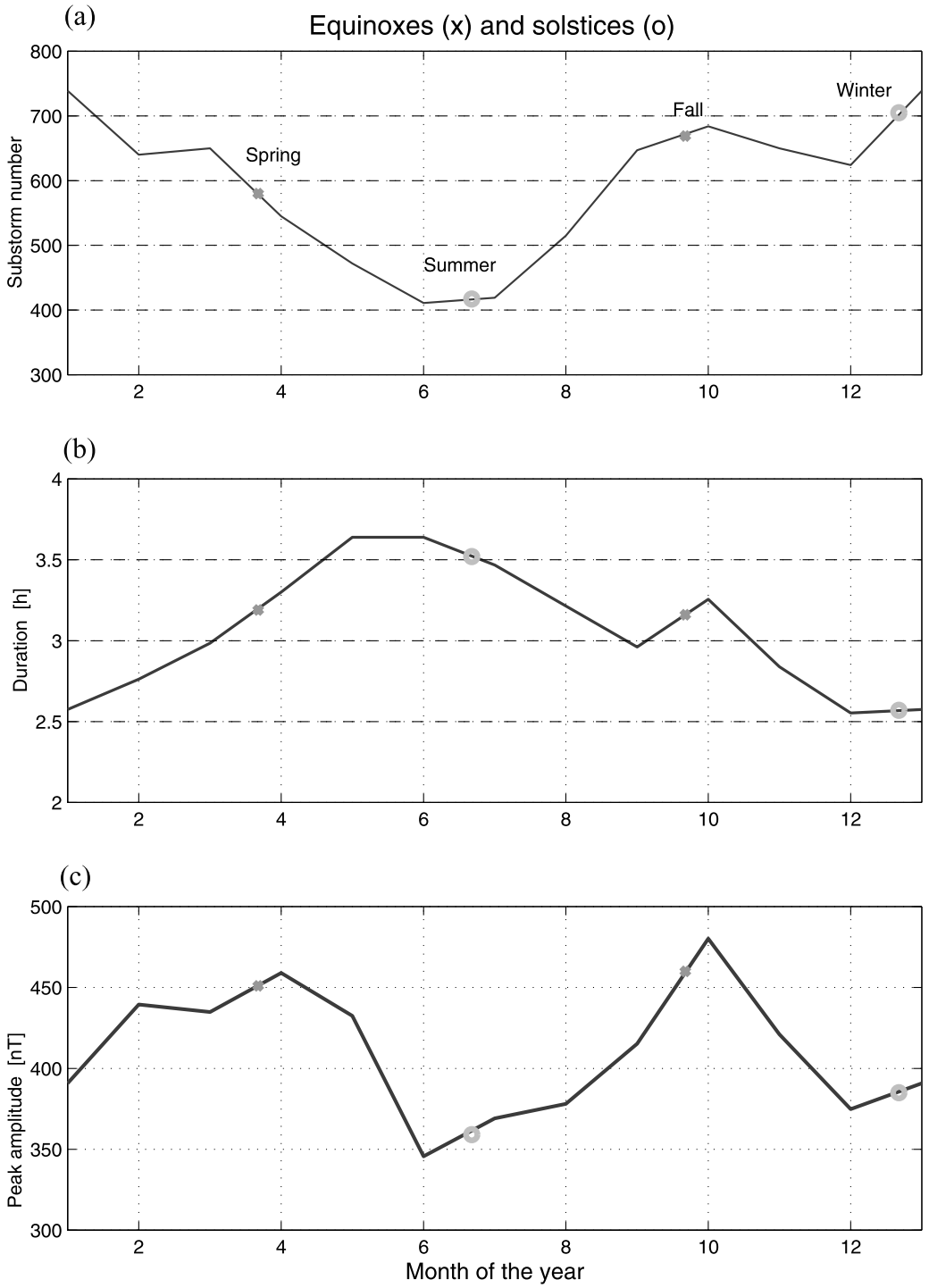

Figure 8. Seasonal variation of (a) the substorm number, (b) the duration, and (c) the substorm strength, i.e., peak amplitude. Summer and winter solstices are marked by circles, and spring and fall equinoxes are marked by crosses.

brightenings in images [*Frey et al.*, 2004], geostationary injections [*Borovsky et al.*, 1993], magnetotail dipolarization [*Slavin et al.*, 1997] and plasma sheet signatures [e.g., *Hones et al.*, 1973]. *Frey et al.* [2004] identified substorm onsets from the FUV instrument on board IMAGE spacecraft. *Frey et al.* [2004] found over 2400 substorms in 2.5 years, which gives about 1000 each year. The number of events in each year from FUV list is in good agreements with our 500 each year, because *Frey et al.* [2004] used entire UT coverage and we used a limited time sector of 1600–0300 UT. The use of a limited UT interval may also has a small influence to the peak amplitude of substorms. Substorms starting close to the 1600 UT or ending close to the 0300 UT are less intense, and possibly slightly shorter, in our statistics than they would be

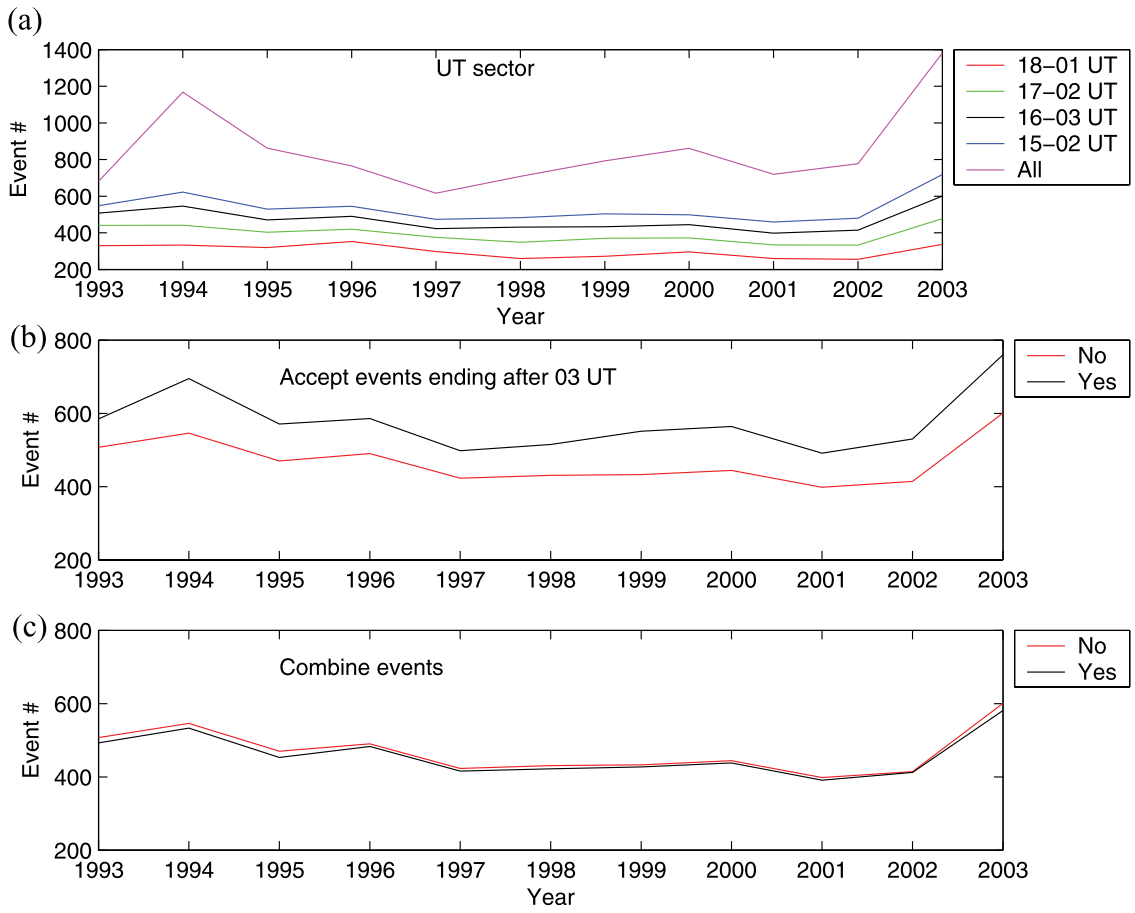

Figure 9. The influence of the use of a limited UT sector on the substorm number R_{SS}. (a) Selected UT sectors: 1800–0100 UT, 1700–0200 UT, 1600–0300 UT, 1500–0200 UT, and all UT hours. (b) Accepting and not accepting events ending after 0300 UT. (c) Effect of combining the substorm to the previous one if the new substorm begins less than 15 min after the end of the previous substorm.

in reality. That is due to the fact that IMAGE magnetometers observe best the times around the local midnight, which is about 2130 UT for IMAGE network. However, by using a dense network with a good latitudinal coverage (e.g., IMAGE) it is possible to detect the real peak amplitude of the substorm, in that particular LT sector.

[32] The substorm identification recipe was tested in several ways. First, we tested the influence of the use of a limited UT interval to the substorm number. We ran the search engine for different UT intervals and found that the yearly trend for substorm number holds. In Figure 9a we show the following UT intervals: 1800–0100 UT (red line), 1700–0200 UT (green line), 1600–0300 UT (black line), 1500–0200 UT (blue line), and all UT sectors (pink line). The trend of getting more substorms during the declining solar cycle phases compared to the other solar cycle phases holds for all tested UT intervals (not all shown in Figure 9). The optimal IMAGE ground-based network coverage is about 1600–0300 UT, which is the one selected to be used in this paper. Furthermore, in this paper we rejected substorms ending after the 0300 UT. In Figure 9b we compare the yearly substorm numbers when rejecting or accepting substorms ending after 0300 UT. In Figure 9c we analyzed the effect of combining/not combining the substorms closer than 15 min apart from each other. The trend in substorm yearly number did not show a big difference whether close substorms were or were not combined.

[33] Second, we tested the substorm identification recipe by varying the minimum substorm duration, minimum peak amplitude, onset drop amount and onset drop time criteria (Figure 10). The yearly substorm number increased only 0.1%, on average, when the minimum duration criteria (Figure 10a) was changed from 15 min to 25 min. The used minimum peak amplitude criteria (Figure 10b) had stronger effect increasing the average yearly substorm number by 114 events (about 20%) when the minimum peak amplitude was changed from 100 nT to 200 nT. Next, the substorm number was computed when the different drop time (10, 15, 20 and 25 min) (Figure 10c) and onset drop amount (60, 80, 100 and 120 nT) (Figure 10d) criteria were used. In all cases, the yearly trend of the substorm number holds and the largest substorm numbers were observed during the declining solar cycle phases. In the original data set, the substorm onset was selected to be when the IL index dropped more than 80 nT in 15 min. The onset drop (in nT) and the onset time, which were used in the final run, were chosen by matching them to the previous data set of visually chosen substorm for 1997 and 1999 [*Tanskanen et al.*, 2002]. Above described tests

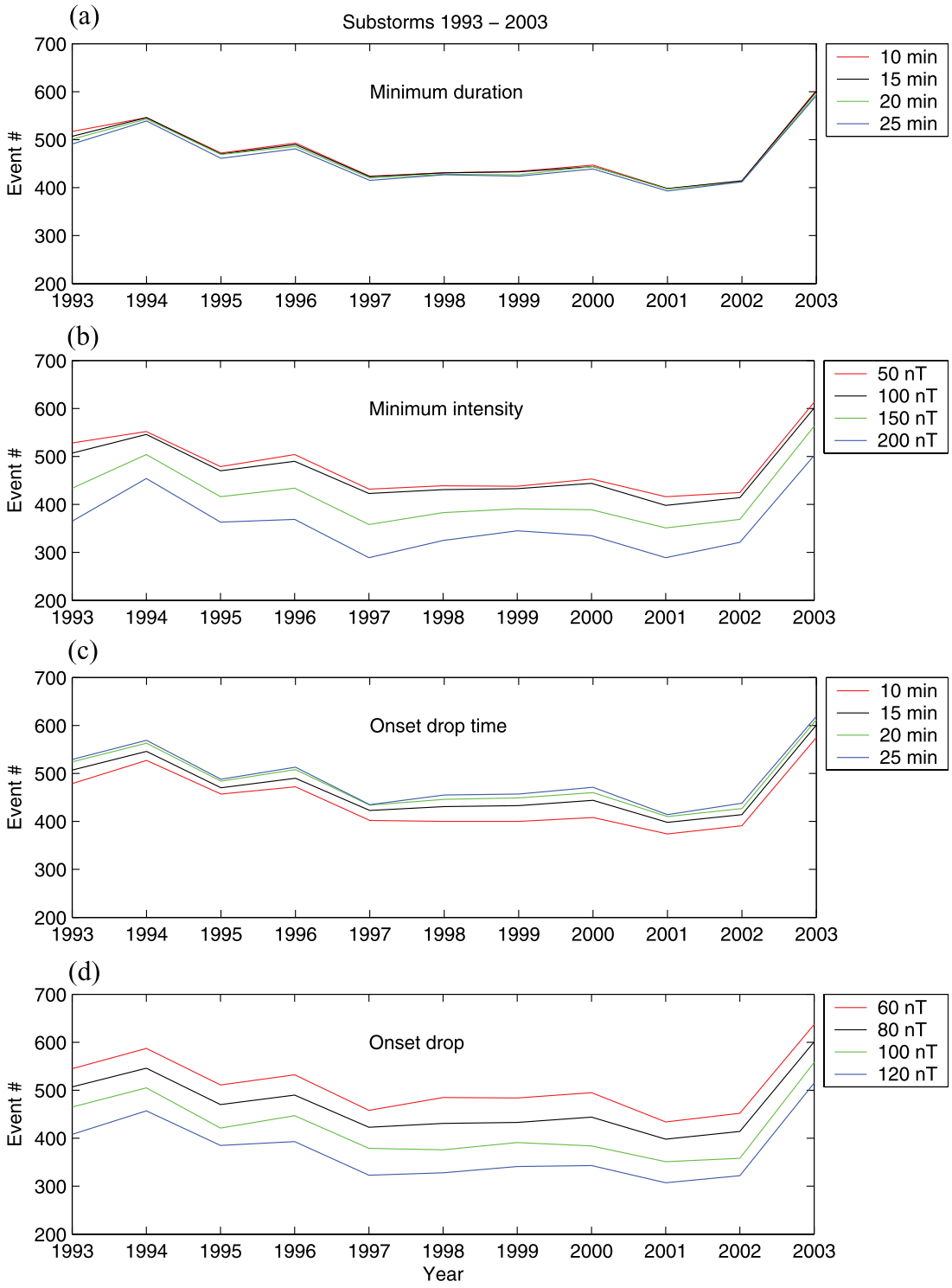

Figure 10. The influence of the different substorm selection criteria to the substorm number R_{SS}. (a) A minimum duration criteria. (b) A minimum peak amplitude criteria. (c) An onset drop time criteria. (d) An onset drop amount criteria.

show that the main results in this paper are qualitatively independent of the search engine search parameters.

8. Conclusions

[34] We identified and analyzed substorms from the beginning of 1993 to the end of 2003. We found 5914 substorm events, with a search engine, that fulfilled the selection criteria described in chapter 2.2. The most intense and the most numerous substorms occurred in 1994 and 2003 coinciding with the time when the high-speed streams frequently hit the Earth. The main results of the study are the following.

[35] 1. A mechanistic method for defining substorms is developed, which enables an algorithmic substorm identifi-

cation by an automated search engine. The identification method was found to be robust and applicable to the ground-based magnetic field measurements to all activity levels, from quiet to extremely intense activity periods.

[36] 2. The measure called the substorm number is formed to describe the occurrence rate of the substorm events over the selected time interval, e.g., a month or a year.

[37] 3. The substorm number and the substorm activity only weakly follow the sunspot number. Almost one fourth of the all identified substorms occurred in 1994 and 2003, which are both during the declining solar cycle phase, 3–4 years after the sunspot maximum. During the year of sunspot maxima in solar cycle 23, the northern hemisphere auroral region was only moderately active.

[38] 4. The typical substorm obtained through the superposed epoch analysis shows a slow increasing trend in an activity level during the substorm growth phase (i.e., the *IL* index decreases) indicating that ionosphere activates already before the substorm onset, during the substorm growth phase.

[39] 5. Substorms last longer during the less active seasons (summer months) and years (1997 and 2001). Furthermore, the substorm number and peak amplitude show much larger values for winter than for summer, which may be partly due the fact that the maximum southward component of the interplanetary magnetic field (B_{south}) occurs in February and minimum in June.

[40] **Acknowledgments.** We wish to thank Ari Viljanen for his help in a baseline selection and Antti J. Tanskanen for carefully reading the manuscript and helping with the programming. We are grateful to James A. Slavin, Tuija I. Pulkkinen, and Kalevi Mursula for fruitful discussions. We thank the institutes who maintain the IMAGE magnetometer array. The work of E.T. was supported by Meltzerfondet and the Academy of Finland.

[41] Wolfgang Baumjohann thanks the reviewers for their assistance in evaluating this paper.

References

Akasofu, S.-I. (1964), The development of the auroral substorms, *Planet. Space Sci.*, *12*, 273.

Baker, D. N., S. G. Kanekal, X. Li, S. P. Monk, J. Goldstein, and J. L. Burch (2004), An extreme distortion of the Van Allen belt from the Halloween solar storm in 2003, *Nature*, *432*, 878.

Bartels, J. (1925), Eine universelle tagesperiode der erdmagnetischen aktivitšt, *Meteorol. Z.*, *42*, 147.

Birkeland, K. (1908), *The Norwegian Aurora Polaris Expedition, 1902–1903*, vol. 1, H. Aschehoug, Oslo.

Borovsky, J. E., R. J. Nemzek, and R. D. Belian (1993), The occurrence rate of magnetospheric-substorm onsets: Random and periodic substorms, *J. Geophys. Res.*, *98*, 3807.

Chapman, S., and J. Bartels (1940), *Geomagnetism*, vol. 1, chap. 11, Oxford Univ. Press, New York.

Cliver, E. W., Y. Kamide, and A. G. Ling (2000), Mountains versus valleys: Semiannual variation of geomagnetic activity, *J. Geophys. Res.*, *105*, 2413.

Cliver, E. W., Y. Kamide, and A. G. Ling (2002), The semiannual variation of geomagnetic activity: Phases and profiles for 130 years of *aa* data, *J. Atmos. Sol. Terr. Phys.*, *64*, 47.

Cortie, A. L. (1912), Sunspots and terrestrial magnetic phenomena, 1898–1911: The cause of the annual variation in magnetic disturbances, *Mon. Not. R. Astron. Soc.*, *73*, 52.

Currie, R. G. (1966), The geomagnetic spectrum—40 days to 5.5 years, *J. Geophys. Res.*, *71*, 4579.

Davis, T. N., and M. Sugiura (1966), Auroral electrojet activity index *AE* and its universal time variations, *J. Geophys. Res.*, *71*, 785.

Durbin, R., S. R. Eddy, A. Krogh, and G. Mitchison (1998), *Biological Sequence Analysis: Probabilistic Models of Proteins and Nucleic Acids*, Cambridge Univ. Press, Cambridge, U. K.

Frey, H. U., S. B. Mende, V. Angelopoulos, and E. F. Donovan (2004), Substorm onset observations by IMAGE-FUV, *J. Geophys. Res.*, *109*, A10304, doi:10.1029/2004JA010607.

Hones, E. W., Jr., J. R. Asbridge, S. J. Bame, and S. Singer (1973), Substorm variations of the magnetotail plasma sheet from $X_{SM} \approx -6\ R_E$ to $X_{SM} \approx -60\ R_E$, *J. Geophys. Res.*, *78*, 109.

Kallio, E. I., T. I. Pulkkinen, H. E. J. Koskinen, A. Viljanen, J. A. Slavin, and K. Ogilvie (2000), Loading-unloading processes in the nightside ionosphere, *Geophys. Res. Lett.*, *27*, 1627.

Kauristie, K., T. I. Pulkkinen, R. J. Pellinen, and H. J. Opgenoorth (1996), What can we tell about auroral electrojet activity from a single meridional magnetometer chain?, *Ann. Geophys.*, *14*, 1177.

Koskinen, H. E. J., and K. E. J. Huttunen (2006), Geoeffectivity of coronal mass ejections, *Space Sci. Rev.*, *124*, 169.

Mayaud, P. N. (1973), A hundred year series of geomagnetic data, 868–1967, indices *aa*, storm sudden commencements, *IAGA Bull. 33*, Int. Union of Geod. and Geophys., Paris.

McPherron, R. I. (1979), Magnetospheric substorms, *Rev. Geophys.*, *17*, 657.

Nevanlinna, H., and E. Kataja (1993), An extension of geomagnetic activity series *aa* for two solar cycles (1844–1868), *Geophys. Res. Lett.*, *20*, 2703.

Nevanlinna, H., and T. I. Pulkkinen (1998), Solar cycle correlation of substorm and auroral occurrence frequency, *Geophys. Res. Lett.*, *25*, 3087.

Newell, P. T., K. Liou, T. Sotirelis, and C.-I. Meng (2001), Auroral precipitation power during substorms: A Polar UV Imager-based superposed epoch analysis, *J. Geophys. Res.*, *106*, 28,885.

Newell, P. T., T. Sotirelis, J. P. Skura, C.-I. Meng, and W. Lyatsky (2002), Ultraviolet insolation drives seasonal and diurnal space weather variations, *J. Geophys. Res.*, *107*(A10), 1305, doi:10.1029/2001JA000296.

Østgaard, N., S. B. Mende, H. U. Frey, J. B. Sigwarth, A. Åsnes, and J. M. Weygand (2007), Auroral conjugacy studies based on global imaging, *J. Atmos. Sol. Terr. Phys.*, *69*, 249.

Richardson, I. G., E. W. Cliver, and H. V. Cane (2000), Sources of geomagnetic activity over the solar cycle: Relative importance of coronal mass elections, high-speed streams, and slow solar wind, *J. Geophys. Res.*, *105*, 18,203.

Rostoker, G., et al. (1995), CANOPUS—A ground-based instrument array for remote sensing the high latitude ionosphere during the ISTP/GGS program, *Space Sci. Rev.*, *71*, 743.

Russell, C. T., and R. L. McPherron (1973), Semiannual variation of geomagnetic activity, *J. Geophys. Res.*, *78*, 92.

Siscoe, G. L. (1980), Evidence in the auroral record for secular solar variability, *Rev. Geophys.*, *18*, 647.

Slavin, J. A., et al. (1997), WIND, GEOTAIL, and GOES 9 observations of magnetic field dipolarization and bursty bulk flows in the near-tail, *Geophys. Res. Lett.*, *24*, 971.

Syrjäsuo, M., and E. Donovan (2004), Diurnal auroral occurrence statistics obtained via machine vision, *Ann. Geophys.*, *22*, 1103.

Syrjäsuo, M., et al. (1998), Observations of substorm electrodynamics using the MIRACLE network, in *Substorms-4*, edited by S. Kokobun and Y. Kamide, p. 111, Terra Sci., Tokyo.

Tanskanen, E., T. I. Pulkkinen, H. E. J. Koskinen, and J. A. Slavin (2002), Substorm energy budget during low and high solar activity: 1997 and 1999 compared, *J. Geophys. Res.*, *107*(A6), 1086, doi:10.1029/2001JA900153.

Tanskanen, E. I., J. A. Slavin, A. J. Tanskanen, A. Viljanen, T. I. Pulkkinen, H. E. J. Koskinen, A. Pulkkinen, and J. Eastwood (2005), Magnetospheric substorms are strongly modulated by interplanetary high-speed streams, *Geophys. Res. Lett.*, *32*, L16104, doi:10.1029/2005GL023318.

Tsurutani, B. T., W. D. Gonzalez, A. L. C. Gonzalez, F. Tang, J. K. Arballo, and M. Okada (1995), Interplanetary origin of geomagnetic activity in the declining phase of the solar cycle, *J. Geophys. Res.*, *100*, 21,717.

Viljanen, A., and L. Häkkinen (1997), IMAGE magnetometer network, in *Satellite-Ground Based Coordination Sourcebook*, edited by M. Lockwood, M. N. Wild, and H. J. Opgenoorth, *Eur. Space Agency Spec. Publ., ESA-SP 1198*, 111.

E. I. Tanskanen, Department of Physics and Technology, University of Bergen, N-5007 Bergen, Norway. (eija.tanskanen@ift.uib.no)